

## **Spectral Characteristics of the Impurity Band in the Structural Disorder Model**

**I. M. Lifshitz,<sup>1</sup> S. A. Gredeskul,<sup>2</sup> and L. A. Pastur<sup>2</sup>**

*Received February 9, 1984*

---

The density and character of the quantum states in the impurity band arising from broadening of the local impurity level are studied. When the impurity concentration is small, the energy levels and states in the impurity band admit an apparent geometric systematics in the main approximation. In this systematics, the wave functions are localized at one or two centers, though the energy levels depend on the positions of other centers. The density of states and the space correlators calculated in the main approximation are of universal nature, i.e., are represented in a certain scale as universal functions independent of the concentration. In the immediate vicinity of the local level, where in terms of the geometric systematics the density of states has a gap, different states become significant, which collectivize a larger number of centers. They fill the gap, the filling degree essentially depending on the impurity concentration. The general structure of the impurity band spectrum is discussed.

---

**KEY WORDS:** Impurity band; structural disorder; density of states; localization; correlating functions.

### **1. INTRODUCTION**

The problem of the nature of the spectrum in the impurity band arising from local impurity level broadening was earlier studied by one of the authors.<sup>(1)</sup> In this paper, following up Ref. 1, we are going, firstly, to describe the method and results of the respective section of Ref. 1 more consistently and from a somewhat different point of view and, secondly, to obtain some new results on the density of states structure and the nature of states at the band center, and also the properties of the density–density correlation function.

---

<sup>1</sup> S. I. Vavilov Institute for Physical Problems, USSR Academy of Science, Moscow, USSR.

<sup>2</sup> Physico-Technical Institute of Low Temperatures, UkrSSR Academy of Sciences, Kharkov, USSR.

The contents of the paper is as follows. In Section 2 we briefly describe the model and derive the basic equation for the excitation spectrum. For low impurity concentration the equation permits us to build up an apparent geometric systematics of the levels and states, which is the subject of Section 3. In Section 4, diagrams are constructed by which the levels and states are classified that are described by the geometric systematics of Section 3. The statistical properties of such diagrams are analyzed in Section 5. Section 6 contains calculation of the density of states in the main approximation corresponding to the geometric systematics; the same approximation is used in Section 7 to obtain an expression for the density-density correlation function. One of the findings of Ref. 1 was the existence of a gap of the density of states at the band center in the main approximation. Section 8 presents a more detailed analysis of the spectrum equation which suggests that the gap in the band center density of states is filled to a large extent and with states which are not given by the geometric systematics. Finally, Section 9 contains a discussion of the general structure of the impurity band spectrum.

## 2. MODEL

We shall proceed from the set of equations<sup>(1,2)</sup>

$$\sum_{k \neq j} x_{jk}^{-1} \exp(-tx_{jk}) \psi_k = \varepsilon \psi_j \quad (1)$$

for “projections”  $\psi_j$  of the electron wave functions  $\psi(\mathbf{x})$  on the one-center states  $\psi(\mathbf{x} - \mathbf{x}_j)$ . Here  $t = k_0 l \gg 1$  is the large parameter of the theory, which is related to the dimensionless impurity concentration  $c$  as  $c = t^{-3}$ ;  $l$  is the mean impurity separation,  $k_0$  is the inverse radius of the one-center states  $\psi^{(0)}(\mathbf{r})$ ,  $\mathbf{x} = \mathbf{r}l^{-1}$  is the dimensionless coordinate,  $\mathbf{x}_j$  are impurity random coordinates, and the energy parameter  $\varepsilon$  is proportional to the distance  $E - E_0$  to the one-center local level  $E_0$ . In the configurations of the general position in this model the separations of the nearest-neighboring centers are of the order of 1:  $x_{jk} = |\mathbf{x}_j - \mathbf{x}_k| \sim 1$  and therefore the main contribution to the density of states is due to the energy range  $|\ln \varepsilon| \sim t \gg 1$ .

Let us first consider the auxiliary problem on the spectrum of an infinite system with a finite number  $N$  of impurities which occupy the volume  $V$ . In the typical situation,  $Nl^3 \sim V$ , and inequalities  $Nl^3 \gg V$  and  $Nl^3 \ll V$  correspond to dense and rarefied fluctuations, respectively. The former are responsible for the spectrum in the region  $|\varepsilon| \gg |\varepsilon(l)|$ , the latter for the states in the immediate vicinity of the local level  $|\varepsilon| \ll |\varepsilon(l)|$  [ $\varepsilon(\mathbf{r})$  is some of pair

levels in an infinite system with two impurities situated at points  $\mathbf{0}, \mathbf{r}$ ]. The equation for the spectrum in the model (1) is as follows:

$$\det \| -\varepsilon \delta_{jk} + (1 - \delta_{jk}) x_{jk}^{-1} \exp(-t x_{jk}) \| = 0 \quad (2)$$

Expansion of this determinant in powers of  $\varepsilon$  gives

$$\varepsilon^N + \sum_{n=2}^N \varepsilon^{N-n} Q_n = 0 \quad (3)$$

The coefficients  $Q_n$  are sums

$$Q_n = \sum_k Q_n^{(k)}(\Gamma_n^{(k)})$$

whose terms are

$$Q_n^{(k)}(\Gamma_n^{(k)}) = (-1)^{j_k} \prod_{m=1}^{j_k} \frac{\exp[-t \mathcal{L}(\Gamma_{p(m)}^{(m)})]}{\mathcal{M}(\Gamma_{p(m)}^{(m)})}$$

$$\sum p(m) = n$$

In these expressions  $\Gamma_n^{(k)}$  is an  $n$ -polygon (generally speaking, multiply connected) with the vertices at  $n$  separate points occupied by the impurities, subscript  $k$  is the number of the individual  $n$ -polygon. Each of them consists of  $j_k$  simple loops  $\Gamma_{p(m)}^{(m)}$  ( $m = 1, 2, \dots, j_k$ ) which are specified by their respective vertices and the order of numbering. Finally,  $\mathcal{L}(\Gamma_{p(m)}^{(m)})$  is the perimeter and  $\mathcal{M}(\Gamma_{p(m)}^{(m)})$  the product of the  $\Gamma_{p(m)}^{(m)}$  loop side lengths.

Such structure of the coefficients  $Q_n$  leads for  $t \rightarrow \infty$  (limiting case of small concentration) to an apparent geometric systematics of levels and states. Considering  $t$  as the largest parameter of the problem, we shall up to Section 8 neglect the extremely small probability degenerate situations of any sort (in particular, those associated with coincidence of perimeters of various  $n$ -polygons  $\Gamma_n^{(k)}$  to within  $t^{-1}$ ). Therefore each of the coefficients  $Q_n$  depends mainly on the contribution of only one  $n$ -polygon  $\Gamma_n$  which has the minimum perimeter, i.e.,

$$Q_n = \kappa_n \exp(-t \tilde{L}_n) \quad (4)$$

where  $\tilde{L}_n$  is, to within the terms of the order of  $t^{-1}$ , the perimeter of the minimum contour  $\Gamma_n$ :

$$\tilde{L}_n \approx L_n = \min_k \mathcal{L}(\Gamma_n^{(k)}) = \mathcal{L}(\Gamma_n)$$

and  $\kappa_n$  is plus or minus unity, according to whether it is an even or odd number of loops that  $\Gamma_n$  having the minimum perimeter consists of. Finally, introducing a new energy variable  $s$ ,

$$\varepsilon = \sigma \exp(-ts), \quad \sigma = \pm 1, \quad s = -t^{-1} \ln |\varepsilon| \quad (5)$$

write Eq. (3) as

$$1 + \sum_{n=2}^N \kappa_n \sigma^n \exp[-t(\tilde{L}_n - ns)] = 0 \quad (6)$$

### 3. GEOMETRIC SYSTEMATICS OF LEVELS AND STATES

For an arbitrary  $s$  value, all the terms in this equation are of different orders of magnitude with respect to the parameter  $e^{-t}$ , and the whole determinant, i.e., the left-hand side of Eq. (6), is nonzero, since it is determined by the only one, maximal, summand (in particular for  $s = 0$ , the first one). As  $s$  increases, the exponents in Eq. (6) grow the more rapidly, the larger  $n$  is. Therefore, if for certain  $s = s_1$  the larger order of magnitude is found in the term containing  $n = n_1$ , then the nearest root  $s_2 > s_1$  of Eq. (6) will appear as soon as any of the exponents of subsequent terms with the number  $n_2 > n_1$  becomes equal to  $t(n_1 s_2 - \tilde{L}_{n_1})$  for the first time. Coincidence of a larger number of exponents is another example of degeneracy. Since it has rather small probability for  $t \gg 1$ , we shall neglect it. Besides, for  $t \rightarrow \infty$ ,  $\tilde{L}_n$  may be identified with the minimum perimeter  $L_n$ . Having the exponents equal, we find  $s_2$ , that is, the absolute value  $|\varepsilon_2|$  of the dimensionless energy, its sign being defined by the respective coefficients  $\kappa_{n_1}, \kappa_{n_2}$  in Eq. (6).

Thus, in variables  $s, \sigma$ , after having passed to the limit  $t \rightarrow \infty$ , we arrive at an apparent geometric systematics of levels and states, specified by a sequence of  $n$ -polygons with minimum perimeters whose vertices are at points where impurities stay. The approximation corresponding to such systematics will below be called main and is the subject of Sections 3–7.

Introduce

$$a_n = L_{n+1} - L_n, \quad 2b_n = L_{n+2} - L_n$$

Then the roots of Eq. (6), as is readily seen, are specified every time by one of the following two relations:

$$s = a_n \quad (\text{I})$$

$$s = b_n \quad (\text{II})$$

representing two cases of appearance of a pair of maximum exponents:

$$(n+1)s - L_{n+1} = ns - L_n \quad (\text{I})$$

$$(n+2)s - L_{n+2} = ns - L_n \quad (\text{II}) \quad (7)$$

There are no more cases, since if two maximum exponents have appeared whose numbers differ by more than 2, then the total number of real roots of Eq. (6) will be smaller than the number of impurities, which is impossible because of the Hermitian character specified by the left-hand side of Eq. (2).

The process of origination of the roots of Eq. (6) may be clearly illustrated geometrically (Fig. 1). Consider a set of points with coordinates  $(n, L_n)$ ,  $n \geq 2$ , and construct, starting from the coordinate origin, a convex envelope of this set  $y(n)$ . Then Eq. (7) means that the envelope vertices abscissas coinciding with the successive numbers of the maximum exponents (for various  $s$  values) do not differ by more than 2.

The first of the possibilities in Eq. (7) is realized when  $a_n < b_n$  and corresponds to the root  $\varepsilon = -(\kappa_{n+1}/\kappa_n) \exp(-ta_n)$  of a certain sign. In this case, polygons  $\Gamma_n$  and  $\Gamma_{n+1}$  differ as a rule by one vertex  $\mathbf{x}_1$  only, and the quantum state corresponding to the level  $\varepsilon$  is localized at the impurity center occupying this vertex:

$$\psi(\mathbf{x}) = \psi^{(0)}(\mathbf{x} - \mathbf{x}_1) \quad (8)$$

The second possibility of Eq. (7) is the case when  $b_n < a_n$ ,  $\sigma_n + \sigma_{n+2} = 0$ , and corresponds to two roots  $\varepsilon_{1,2} = \pm \exp(-tb_n)$ . In this case, polygons  $\Gamma_n$  and  $\Gamma_{n+2}$  contain different parity numbers of simple loops  $\sigma_{n+2} = -\sigma_n$  and differ only by two vertices,  $\mathbf{x}_1$  and  $\mathbf{x}_2$ , and the corresponding states are collectivized between the two centers located at these points:

$$\psi(\mathbf{x}) = 2^{-1/2} [\psi^{(0)}(\mathbf{x} - \mathbf{x}_1) \pm \psi^{(0)}(\mathbf{x} - \mathbf{x}_2)] \quad (9)$$

Note that after a state has appeared at a center [for the first possibility of (7)] or a pair of centers (the second one), the centers are excluded from the subsequent classification of states, because otherwise, even in the zero-order approximation with respect to  $e^{-t}$  corresponding to the geometric systematics, the orthogonality of the eigenstates of the Hamiltonian for the system (1) would be violated.

The minimum contours  $\Gamma_n$  with  $n$  vertices, with probability close to 1, consist of loops with small numbers of vertices (biangles, triangles, sometimes pentagons, etc.). In particular, simple loops  $\Gamma_{2m}$  with  $m > 1$  do not exist, because such a loop would always be able to be broken down into a number of biangles of a smaller perimeter. In the one-dimensional case, contours  $\Gamma_n$  always consist of biangles and triangles whose vertices are nearest neighbors.

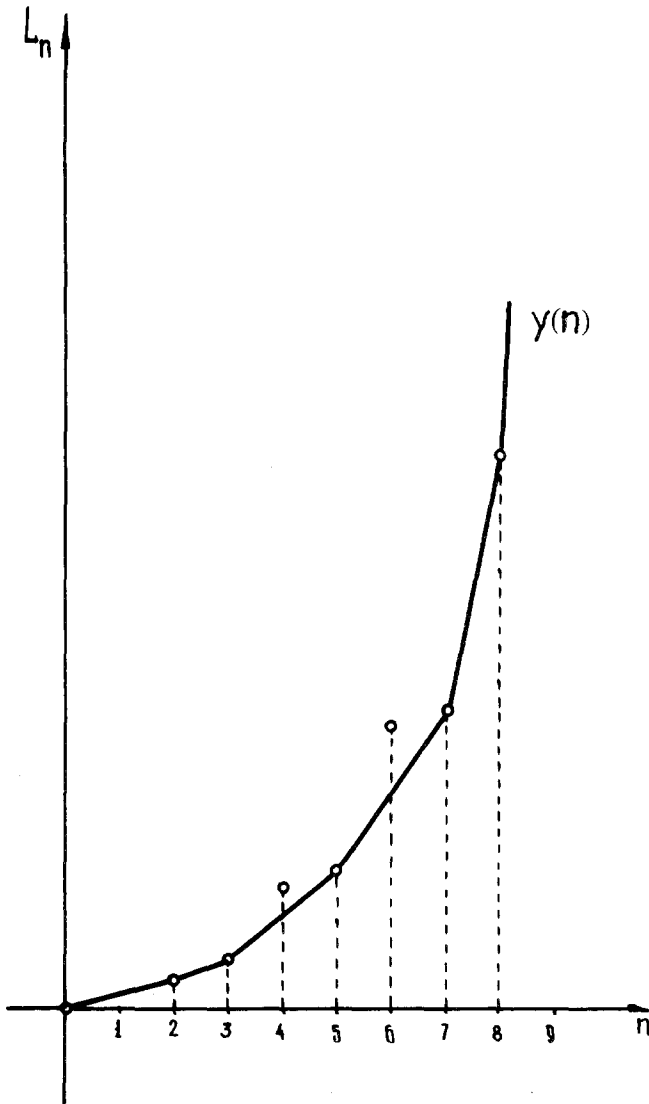


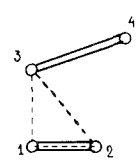
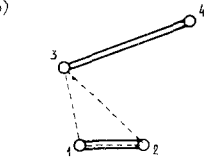
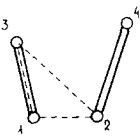
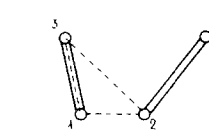
Fig. 1

In the general case, the energy levels in the logarithmic scale, as follows from Eq. (7), are given by such formulas as

$$s = \sum \alpha_{ij} x_{ij}, \quad \sum \alpha_{ij} = 1 \quad (10)$$

$$\alpha_{ij} = \begin{cases} 0, \pm 1, \pm 2 & \text{(I)} \\ 0, \pm \frac{1}{2}, \pm 1 & \text{(II)} \end{cases}$$

Table I.

|  |  |   |
|--|--|---|
| $L_2 = 2x_{12} = 2b_0$<br>$L_3 = x_{12} + x_{23} + x_{13}$<br>$a_2 = x_{23} + x_{13} - x_{12}$<br>$\sigma_2 = \sigma_3 = -\sigma_4 = -1$<br>$\varepsilon_{3,2} = \pm 2^{\frac{1}{2}}(\psi^{(1)} \pm \psi^{(2)})$<br>$\psi_{1,2} = \exp(-tb_0)$ | $b_2 < a_2$<br>$\varepsilon_{3,4} = \pm \exp(-tb_2)$<br>$\psi_{3,4} = 2^{-\frac{1}{2}}(\psi^{(3)} \pm \psi^{(4)})$ | $b_2 > a_2$<br>$\varepsilon_3 = -\exp(-ta_2), \quad \psi_3 = \psi^{(3)}$<br>$\varepsilon_4 = +\exp(-ta_3), \quad \psi_4 = \psi^{(4)}$ |
| $L_4 = 2(x_{12} + x_{34})$<br>$b_2 = x_{34}$<br>$a_3 = 2x_{34} + x_{12} - x_{13} - x_{23}$   | a)                                | b)   |
| $L_4 = 2(x_{13} + x_{24})$<br>$b_2 = x_{13} + x_{24} - x_{12}$<br>$a_3 = 2x_{24} + x_{13} - x_{12} - x_{23}$   | c)                                | d)   |

Particular  $\alpha_{ij}$  values in each case depend on the structures of minimum contours with  $n$  and  $n + p$  ( $p = 1, 2$ ) vertices.

The above statements are suitable to be illustrated by a comparatively simple, though nontrivial, example of a four-center system. Squares (a)–(d) of Table I contain four variants of arrangement of four impurities corresponding to various  $n$ -polygons  $\Gamma_n$  and various inequalities between  $a_2$  and  $b_2$ . The left-hand uppermost square shown information for all the four cases. All the rest of the left-hand (upper) squares refer to the respective rows (columns) of the table.

#### 4. DIAGRAMS

Turning to the general classification of levels and states, it is appropriate to note first of all that, when the configuration of all the  $N$  centers (i.e., points  $x_1, \dots, x_N$ ) is given, then the structures of all the contours  $\Gamma_n$  having the minimum perimeters  $L_n$  are uniquely predetermined. Thereby the sequence  $\{L_n\}$  of minimum perimeters which are ordinates of the vertices of the convex envelope in Fig. 1 is uniquely predetermined, as well as all the energy levels and wave functions. For any transition  $L_n \rightarrow L_{n+1}$  or  $L_n \rightarrow L_{n+2}$  rearrangement of the minimum contours amounts to rearrangement of a few closely spaced loops. Thus, the minimum contour  $\Gamma_n$

for each of the cases of rearrangement  $\Gamma_n \rightarrow \Gamma_{n+1}$  or  $\Gamma_n \rightarrow L_{n+2}$  breaks down into the nonrearranging part  $\Gamma_{n-m}$  and the rearranging part  $\Gamma_m^* \rightarrow \Gamma_{m+1}^*$  or  $\Gamma_m^* \rightarrow \Gamma_{m+2}^*$  (here  $m$  is the number of rearranging vertices of the  $n$ -polygon  $\Gamma_n$ , and  $\Gamma_m^*$  the minimum contour based on these vertices). The minimum perimeters accordingly consists of two terms:  $L_n = L_{n-m} + L_m^*$ . Therefore, irrespective of the number  $n$ , we may build up the classification on the basis of the number of rearranging vertices  $m$  and the structure of rearranging contours. Such classification of levels and states may be represented by means of diagrams, such as are presented in Tables II and III for  $a_m < b_m$  and  $a_m > b_m$ , respectively, where  $a_m = L_{m+1}^* - L_m^*$ ,  $2b_m = L_{m+2}^* - L_m^*$ . The number of rearranging vertices  $m + 1$  or  $m + 2$  will be called the diagram order,  $k$ . The black circles label the vertices at which the appropriate quantum state is localized. The spectrum description based on such diagrams is universal and does not depend on  $n$  or  $N$ . It is only the nonrearranging contour parts  $\Gamma_{n-m}$ , indicated by a large circle, that is dependent on these quantities; it has no influence on the systematics of levels and states.

In order to distinguish between the diagrams, let us introduce the diagram-characterizing symbol  $\mathfrak{R}$ , including the diagram type, order, and perhaps an additional index to indicate topologically nonequivalent diagrams of the same type and order. Introduce also for each diagram  $\mathfrak{R}$  a certain order of numbering of the rearranging vertices, so that the quantum state for type I diagrams should always be localized at the center  $x_1$  and that for type II diagrams should be collectivized between centers  $x_1$  and  $x_2$ . Such denumeration will henceforth be referred to as standard (such as in particular the denumeration of vertices in Tables II and III).



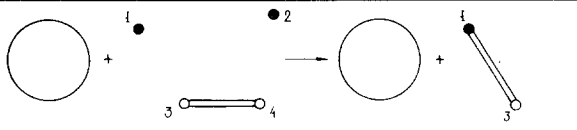
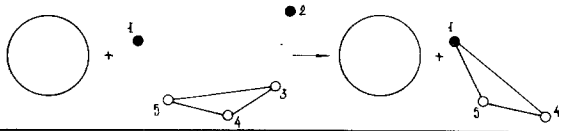
In terms of such diagrams, the spectrum of the four-center system for configurations (a) and (c) in Table I is associated with transitions  $\Gamma_0 \rightarrow \Gamma_2$ ,

Table II.

| $k = m + 1$ | $\bigcirc + \Gamma_m^* \longrightarrow \bigcirc + \Gamma_{m+1}^*$ | $S = \alpha_m$                       |
|-------------|---|--------------------------------------|
| 3           |   | $x_{21} + x_{13} - x_{23}$           |
| 4           |   | $2x_{15} + x_{42} - x_{43} - x_{25}$ |
| ...         | ...   | ...                                  |



Table III.

|                  |   |  |
|------------------|---|--|
| $\kappa = m + 2$ |  | $S = b_m$  |
| 2                |  | $\propto \chi_{12}$  |
| 4                |  | $\propto \chi_{13} + \chi_{24} - \chi_{34}$                                      |
| 5                |  | $\propto \chi_{34} + \frac{1}{2}(\chi_{13} + \chi_{24} - \chi_{34} - \chi_{14})$ |
| ...              | ...   | ...  |

$\Gamma_2 \rightarrow \Gamma_4$ ; the transition  $\Gamma_0 \rightarrow \Gamma_2$  in both the cases and  $\Gamma_2 \rightarrow \Gamma_4$  in the case (a) correspond to diagram II2 (type II, order 2, see Table III), while the transition  $\Gamma_2 \rightarrow \Gamma_4$  for (c) corresponds to diagram II4. For configurations (b) and (d), transitions  $\Gamma_0 \rightarrow \Gamma_2$ ,  $\Gamma_2 \rightarrow \Gamma_3$ ,  $\Gamma_3 \rightarrow \Gamma_4$  are realized, corresponding to diagrams II2, I3, I4, respectively; the difference between the two configurations appears only in the  $\varepsilon$  level magnitude. The expressions for  $a_{2,3}$  and  $b_{0,2}$  in Table I, as well as the right-hand columns of Tables II and III, are examples of the general equation (10) in these special situations.

Note a specific feature of the states represented by type II diagrams. In both the cases the wave function (to within exponentially small corrections, which are neglected in the geometric systematics) is localized around two centers included in  $\Gamma_{m+2}^*$  and not  $\Gamma_m^*$ . Collectivized are states between comparatively distant centers (e.g., 1 and 2 for diagrams II4 and II5), while the other centers make practically no contribution to  $\psi$ . At the same time, the energy levels are specified by the difference  $L_{m+2}^* - L_m^*$  including a larger number of separations. This situation is somewhat similar to that in the periodical structure in the tight-binding approximation: wave function overlapping for nearest centers causes collectivization of states at larger distances where no direct tunneling is possible. However, the probability of pairing of distant centers by virtue of higher-order diagrams numerically decreases rapidly with increasing diagram order.

Till now we have considered the auxiliary problem of determination of the spectrum of an infinite system with a finite number  $N$  of impurities whose volume is of the order of  $V$ . However, the above systematics of levels

and states is valid also for a system with an infinite number of impurities with the average separation  $l$ . The physical sense of this is very simple: for large  $N$  and  $V$  values, random coincidence of distances  $x_{ij} \approx x_{i'j'} \sim 1$  between pairs of impurities situated far apart in the space,  $x_{ii} \gg 1$  does not affect the states localized in the respective regions of space (this is a manifestation of the additivity of the density of states and their localization). In terms of our systematics, this fact means that rearrangement of contours situated in the same region of space is not affected by the "occupied" vertices situated in remote regions and indicates the origin of factorization of the left-hand part of Eq. (6). Therefore, for the typical configuration, the problem of determination of the spectrum of a system with an infinite number of impurities reduces to an infinite number of auxiliary problems with finite (and seemingly small) number of centers.

## 5. PROBABILITIES

Each configuration of impurity centers  $\{\mathbf{x}_1, \dots, \mathbf{x}_N\}$  is characterized by the contour sequence  $\{I_n\}$  with minimum perimeters  $L_n$  and a sequence of diagrams  $\{\mathfrak{R}_n\}$  responsible for the spectrum (in increasing order of  $s$ ) and the states. Note that since the centers have already received certain numbers, denumeration of vertices within each diagram differs from the standard denumeration introduced in Section 4.

Divide the whole configurational space into regions  $\Delta I_i$ , so that within each of them the spectrum and the states should be realized on the same sequence of diagrams with the vertices denumeration conserved within each diagram. Then the average of any function  $\langle f(\mathbf{x}_1, \dots, \mathbf{x}_N) \rangle$  is<sup>3</sup>

$$N^{-N} \int f(\mathbf{x}_1, \dots, \mathbf{x}_N) d\mathbf{x}_1 \cdots d\mathbf{x}_N = \sum_i N^{-N} \int_{\Delta I_i} f(\mathbf{x}_1, \dots, \mathbf{x}_N) d\mathbf{x}_1 \cdots d\mathbf{x}_N \quad (11)$$

Let us now consider calculation of the mean value of a certain physical quantity  $F$  which has in each realization the form of a sum of contributions of all the diagrams to determine the spectrum

$$F = \sum_n F_{\mathfrak{R}_n} \quad (12)$$

Let a certain diagram  $\mathfrak{R}$  of the  $k$ th order appear  $p_i(\mathfrak{R})$  times in the sequence of diagrams  $\{\mathfrak{R}_n\}_i$  specified by the region  $\Delta I_i$ , and  $\mathbf{x}_{m_j}^{(i)}$ ,

<sup>3</sup> Recall that the volume of the system in the  $\mathbf{x}$  space is  $N$ .

$1 \leq l \leq p_i(\mathfrak{R})$  be the coordinates of the rearranging vertices involved. Then the contribution to the average value  $\langle F \rangle$  due to all the  $\mathfrak{R}$  diagrams is

$$\langle F \rangle_{\mathfrak{R}} = \sum_i N^{-N} \sum_{l=1}^{p_i(\mathfrak{R})} \int_{\Delta\Gamma_i} F(\mathbf{x}_{m_1}^{(l)}, \dots, \mathbf{x}_{m_k}^{(l)}) d\mathbf{x}_1 \cdots d\mathbf{x}_N \quad (13)$$

Each term, after integration over the variables which do not enter into the integrand, may be written as

$$N^{-N} \int_{\Delta\Gamma_{il}(\mathfrak{R})} S_i(\mathbf{x}_{m_1}^{(l)}, \dots, \mathbf{x}_{m_k}^{(l)}) F(\mathbf{x}_{m_1}^{(l)}, \dots, \mathbf{x}_{m_k}^{(l)}) d\mathbf{x}_{m_1}^{(l)} \cdots d\mathbf{x}_{m_k}^{(l)}$$

where  $\Delta\Gamma_{il}(\mathfrak{R})$  is the projection of the  $\Delta\Gamma_i$  region onto the subspace  $\{\mathbf{x}_{m_1}^{(l)}, \dots, \mathbf{x}_{m_k}^{(l)}\}$  and  $S_i(\mathbf{x}_{m_1}^{(l)}, \dots, \mathbf{x}_{m_k}^{(l)})$  the volume of the section of the region  $\Delta\Gamma_i$  by a hyperplane corresponding to the fixed coordinate values,  $\mathbf{x}_{m_1}^{(l)}, \dots, \mathbf{x}_{m_k}^{(l)}$ .

Now adopt the standard denumeration of vertices, i.e., substitute  $\mathbf{x}_{m_j}^{(l)} \rightarrow \mathbf{x}_j$  and introduce the indicator function

$$\chi_{il}^{(\mathfrak{R})}(\mathbf{x}_1, \dots, \mathbf{x}_k) = \begin{cases} 1, & (\mathbf{x}_1, \dots, \mathbf{x}_k) \in \Delta\Gamma_{il}(\mathfrak{R}) \\ 0, & (\mathbf{x}_1, \dots, \mathbf{x}_k) \notin \Delta\Gamma_{il}(\mathfrak{R}) \end{cases}$$

Then the contribution of Eq. (13) becomes

$$\langle F \rangle_{\mathfrak{R}} = \int \tilde{P}_{\mathfrak{R}}(\mathbf{x}_1, \dots, \mathbf{x}_k) F(\mathbf{x}_1, \dots, \mathbf{x}_k) d\mathbf{x}_1 \cdots d\mathbf{x}_k \quad (14)$$

where the function  $\tilde{P}_{\mathfrak{R}}(\mathbf{x}_1, \dots, \mathbf{x}_k)$  is determined by relation

$$\tilde{P}_{\mathfrak{R}}(\mathbf{x}_1, \dots, \mathbf{x}_k) = N^{-N} \sum_i \sum_{l=1}^{p_i(\mathfrak{R})} S_i(\mathbf{x}_1, \dots, \mathbf{x}_k) \chi_{il}^{(\mathfrak{R})}(\mathbf{x}_1, \dots, \mathbf{x}_k) \quad (15)$$

(note that for type II diagrams it is a symmetric function of the two first arguments  $\mathbf{x}_1$  and  $\mathbf{x}_2$ ).

For translation invariant function  $F$ , Eq. (14) becomes as follows:

$$\langle F \rangle_{\mathfrak{R}} = \frac{N}{g_{\mathfrak{R}}} \int P_{\mathfrak{R}}(\Gamma_{\mathfrak{R}}) F(\Gamma_{\mathfrak{R}}) d\Gamma_{\mathfrak{R}} \quad (16)$$

Here  $\Gamma_{\mathfrak{R}} = \{\mathbf{x}_2, \dots, \mathbf{x}_k\}$ ,  $g_{\mathfrak{R}}$  is the number of the levels generated by the  $\mathfrak{R}$  diagram, i.e.,

$$g_{\mathfrak{R}} = \begin{cases} 1 & \text{(I)} \\ 2 & \text{(II)} \end{cases} \quad (17)$$

and the functions  $P_{\mathfrak{R}}(\Gamma_{\mathfrak{R}})$  are

$$P_{\mathfrak{R}}(\Gamma_{\mathfrak{R}}) = \frac{g_{\mathfrak{R}}}{N} \int \tilde{P}_{\mathfrak{R}}(\mathbf{x}_1, \mathbf{x}_2 + \mathbf{x}_1, \dots, \mathbf{x}_k + \mathbf{x}_1) d\mathbf{x}_1 \quad (18)$$

The quantities

$$p_{\mathfrak{R}} = \int P_{\mathfrak{R}}(\Gamma_{\mathfrak{R}}) d\Gamma_{\mathfrak{R}} > 0 \quad (19)$$

satisfy the normalization relation

$$\sum_{\mathfrak{R}} p_{\mathfrak{R}} = 1 \quad (20)$$

(here summation is over all the diagrams) and therefore may be termed the realization probabilities of  $\mathfrak{R}$  diagrams. The numerical experiments of I. M. Lifshitz and I. V. Masanski (unpublished) for a system of eight centers yield  $p_{\mathfrak{R}}$  probabilities listed in Table IV. It is seen that 94% of all states are given by the first four diagrams of Tables II and III.

Let us see how the above functions  $\tilde{P}_{\mathfrak{R}}$  and  $P_{\mathfrak{R}}$  used for the averaging depend on  $N$ . Equations (19) and (20) show that the probabilities  $p_{\mathfrak{R}}$  and their densities  $P_{\mathfrak{R}}(\Gamma_{\mathfrak{R}})$  remain finite when  $N \rightarrow \infty$ . But then Eq. (18) means that for  $N \rightarrow \infty$  the integrand  $\tilde{P}_{\mathfrak{R}}$  is independent of  $\mathbf{x}_1$ , whence

$$P_{\mathfrak{R}}(\Gamma_{\mathfrak{R}}) = g_{\mathfrak{R}} \tilde{P}_{\mathfrak{R}}(\mathbf{0}, \mathbf{x}_2, \dots, \mathbf{x}_k) \quad (21)$$

or

$$\tilde{P}_{\mathfrak{R}}(\mathbf{x}_1, \mathbf{x}_2, \dots, \mathbf{x}_k) = g_{\mathfrak{R}}^{-1} P_{\mathfrak{R}}(\mathbf{x}_{21}, \dots, \mathbf{x}_{k1}) \quad (22)$$

Finally, we obtain for the average value of the quantity  $F$  of Eq. (12), by summation over all the various diagrams:

$$\langle F \rangle = \sum_{\mathfrak{R}} \int \tilde{P}_{\mathfrak{R}}(\mathbf{x}_1, \dots, \mathbf{x}_k) F(\mathbf{x}_1, \dots, \mathbf{x}_k) d\mathbf{x}_1 \cdots d\mathbf{x}_k \quad (23)$$

and for the case of translation invariant function  $F$ ,

$$\langle F \rangle = N \sum_{\mathfrak{R}} g_{\mathfrak{R}}^{-1} \int P_{\mathfrak{R}}(\Gamma_{\mathfrak{R}}) F(\Gamma_{\mathfrak{R}}) d\Gamma_{\mathfrak{R}} \quad (24)$$

Table IV.

|                    |        |        |        |        |
|--------------------|--------|--------|--------|--------|
| $\mathfrak{R}$     | II2    | I3     | I4     | II4    |
| $P_{\mathfrak{R}}$ | 0,6489 | 0,1675 | 0,0798 | 0,0442 |

## 6. DENSITY OF STATES IN THE MAIN APPROXIMATION

In the variables  $s, t$ , the density of states  $\rho_\sigma(s, t)$  normalized to the unit volume in the  $\mathbf{x}$  space is

$$\rho_\sigma(s, t) = N^{-1} \sum_m \delta_{\sigma\sigma_m} \delta(s - s_m)$$

$$\sum_\sigma \int_0^\infty \rho_\sigma(s, t) ds = 1$$

When  $t \rightarrow \infty$ , the energy levels and states are described by the geometric systematics of Section 3. Therefore the maximum density of states is a universal  $t$ -independent function:

$$\rho_\sigma(s) = \lim_{t \rightarrow \infty} \rho_\sigma(s, t), \quad \sum_\sigma \int_0^\infty \rho_\sigma(s) ds = 1 \quad (25)$$

and for each realization may be represented as a sum over the diagrams entering into the sequence  $\{\mathfrak{R}_n\}$  defining the spectrum

$$\rho_\sigma(s) = N^{-1} \left[ \sum_n^{\text{I}} \delta_{\sigma\sigma_n} \delta(s - s_n) + \sum_n^{\text{II}} \delta(s - s_n) \right] \quad (26)$$

(the symbol above  $\sum$  indicates the type of diagrams over which summation is carried out). In other words,  $\rho_\sigma(s)$  has the form of Eq. (12), and the associated functions  $F_{\mathfrak{R}_n}$  are

$$F_{\mathfrak{R}_n} = \begin{cases} N^{-1} \delta_{\sigma\sigma_{\mathfrak{R}_n}} \delta(s - s_{\mathfrak{R}_n}) & \text{(I)} \\ N \delta(s - s_{\mathfrak{R}_n}) & \text{(II)} \end{cases} \quad (27)$$

The levels  $s_{\mathfrak{R}_n}$  in these equations are defined by Eqs. (10) invariant with respect to simultaneous translation of all coordinates. Allowing for the self-averageness of the density of states, we find from Eq. (26), by using Eqs. (27) and (26), that

$$\rho_\sigma(s) = \rho_\sigma^{\text{I}}(s) + \rho_\sigma^{\text{II}}(s)$$

$$\rho_\sigma^{\text{I}}(s) = \sum_{\mathfrak{R}}^{\text{I}} \delta_{\sigma\sigma_{\mathfrak{R}}} \int P_{\mathfrak{R}}(\Gamma_{\mathfrak{R}}) \delta[s - s(\Gamma_{\mathfrak{R}})] d\Gamma_{\mathfrak{R}} \quad (28)$$

$$\rho_\sigma^{\text{II}}(s) = \frac{1}{2} \sum_{\mathfrak{R}}^{\text{II}} \int P_{\mathfrak{R}}(\Gamma_{\mathfrak{R}}) \delta[s - s(\Gamma_{\mathfrak{R}})] d\Gamma_{\mathfrak{R}}$$

(summations over *all* the different diagrams).

As follows from the equations, in order to find the density of states, one has to construct the functions  $P_{\mathfrak{R}}(\Gamma_{\mathfrak{R}})$ , which is not an easy thing to do. However, based on simple reasons, we can judge on the behavior of  $\rho_{\sigma}(s)$  in regions of small and large  $s$  values and also derive an interpolation formula to describe the  $\rho_{\sigma}(s)$  behavior on the whole spectrum.

Small  $s$  values correspond to relatively large  $\varepsilon$ ,  $|\varepsilon| \gg |\varepsilon(l)|$ . Such levels, clearly, are due to closely spaced pairs of impurities, when two centers are at a distance  $r \ll l$  ( $x \ll 1$ ), and the other nearest neighbors are situated at distances of the order of the average distance from this pair. Such fluctuations have small probability and are therefore separated very far. Therefore the whole volume occupied by the system may be divided into parts, each containing one such fluctuation only. Then, in terms of the auxiliary problem in Section 2, in each of the parts these levels result from the transition  $L_0 \rightarrow L_2$ , where the first and the second terms of the expansion (6) are largest, and they correspond to the diagram of the II2 type in Table III; the nonarranging part marked with a large circle contains no impurity centers at all. A sufficient condition of realization of the II2 diagram in this particular case is the requirement that two centers should be spaced by  $|\mathbf{x}_2| = x$  and be nearest neighbors, that is, that in the volume  $v = \frac{9}{4}\pi x^3$  of the union of the two spheres with radii  $x$  and centers at the two impurities there should be no other impurities. The probability of such event  $p_{\text{II2}}^0$  is obviously not in excess of the probability  $p_{\text{II2}}$ .

The quantities  $P_{\mathfrak{R}}(\Gamma_{\mathfrak{R}})$ , as is evident from their definitions (see Section 5), are probability densities calculated on the condition that the center  $\mathbf{x}_1$  is at the coordinate origin, whence the probabilities  $p_{\mathfrak{R}}$  must be subject to the same condition of calculation. Thus, the probability  $p_{\text{II2}}^0$  of the event discussed in the previous paragraph may be represented as

$$\begin{aligned} p_{\text{II2}}^0 &= \int_0^{\infty} dx \int \frac{(N-v)^{N-2}}{N^{N-1}} N \delta(|\mathbf{x}_2| - x) d\mathbf{x}_2 \\ &= \int_0^{\infty} e^{-v(x)} 4\pi x^2 dx = \int e^{-v(\mathbf{x})} d\mathbf{x} \end{aligned} \quad (29)$$

$$v(\mathbf{x}) = \frac{9}{4}\pi x^3$$

and has the magnitude

$$p_{\text{II2}}^0 = \frac{16}{27} \quad (30)$$

The corresponding probability density  $P_{\text{II2}}^0(\mathbf{x}_2)$  is, as follows from Eq. (29),

$$P_{\text{II2}}^0(\mathbf{x}_2) = \exp\left(-\frac{9\pi}{4} x_2^3\right)$$

and the contribution of such diagram to the density of states, according to Eq. (28), is

$$\rho_{\text{II2}}^0(s) = 2\pi s^2 \exp\left(-\frac{9}{4}\pi s^3\right) \quad (31)$$

For small  $s \ll 1$  this contribution is predominant, since the probability of occurrence of additional built-up centers in the volume  $v(s)$  is exceedingly small. Therefore, for  $s \ll 1$ ,

$$\rho_\sigma(s) \approx \rho_\sigma^{\text{II}}(s) \approx \rho_{\text{II2}}^0(s), \quad s \ll 1$$

If, alternatively,  $s$  is not small, then  $\rho_{\text{II2}}^0(s)$  is the contribution to  $\rho_\sigma(s)$  of the type II2 diagrams in the special case under consideration (in the general situation, within the volume  $v$  there may be other, earlier built-up centers) to which now the transitions  $L_n \rightarrow L_{n+2}$  with  $n \geq 0$  correspond. Note, however, that the contribution of only such diagrams coinciding with the probability  $\rho_{\text{II2}}^0$  is enough to provide almost 2/3 of the density integral.

To large  $s$  values, by Eq. (7), correspond large magnitudes of differences  $L_{n+1} - L_n$  or  $L_{n+2} - L_n$ . Such values may be realized at the rarefied fluctuations, when one or two centers are separated from their nearest neighbors by distances of the order of  $s$ . Such fluctuations have very small probability and, as in the preceding case of dense fluctuations, are spaced very widely, so that the whole volume occupied by the system may be subdivided into parts, each containing only one such fluctuation. Then, in terms of the auxiliary problem, in each of the parts these levels result from the transition  $L_{N-1} \rightarrow L_N$  when the largest are the two last terms of expansion (6), and correspond to a certain type I diagram.<sup>4</sup> Because  $s \gg 1$ , there arises a quasi-one-dimensional situation for such diagrams. Figure 2 shows the right-hand part of the I3 diagram. The wave function is localized at the center  $\mathbf{x}_1$  well away from its neighbors (in a sphere of radius  $x_{12}$  with the center at the point  $\mathbf{x}_1$  there are no other impurities). For the  $s$  level, we obtain

$$s = x_{12} - x_{23} + x_{13} = 2x_{12} - 2x_{23} \sin^2 \frac{\vartheta}{2}, \quad x_{23} \sim 1$$

whence

$$x_{12} = \frac{s}{2} [1 + \mathcal{O}(s^{-1})] \quad (32)$$

<sup>4</sup> The other possibility, associated with the transition  $L_{N-2} \rightarrow L_N$  and type II diagrams, corresponds, for the same  $s$  value, to rarefied fluctuations of an essentially larger volume, and therefore the probability of its realization is negligible.

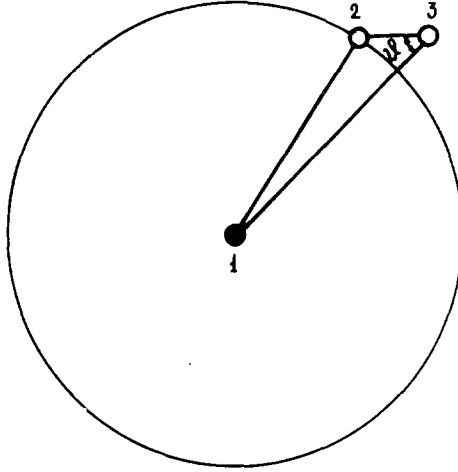


Fig. 2

A sufficient condition of realization of this type of diagrams for  $s \gg 1$  is the requirement that the sphere under discussion should contain no other impurities. The probability density, with logarithmic accuracy, may be found similar to Eq. (31) [we have only to take  $v(\mathbf{x})$  equal to  $\frac{4}{3}\pi x^3$ ] and therefore the density of states appears to be

$$\rho_\sigma(s) \approx \rho_\sigma^1(s), \quad \ln \rho_\sigma(s) \approx -\frac{4\pi}{3} \left(\frac{s}{2}\right)^3, \quad s \gg 1$$

By uniting this result with Eq. (31), we arrive at the interpolation formula

$$\rho_\sigma(s) = 2\pi s^2 \exp[-s^3 \mu_\sigma(s)]$$

where the smooth function  $\mu_\sigma(s) \sim 1$  ranges from  $9\pi/4 = \mu_\sigma(0)$  for small  $s$  values to  $\pi/6 = \lim_{s \rightarrow \infty} \mu_\sigma(s)$ .

Figure 2 shows that the dependence  $x_{12}(s)$  (32) is the same for any dimension  $d$ , and thus,

$$\ln \rho_\sigma(s) = -\omega_d \left(\frac{s}{2}\right)^d, \quad s \gg 1 \quad (33)$$

where  $\omega_d = \pi^{d/2}/\Gamma(1 + d/2)$  is the volume of the  $d$ -dimensional unit sphere. The density of states  $\rho^0(\varepsilon)$  corresponding to  $\rho_\sigma(s)$  is specified by the straightforward relation

$$\rho^0(\varepsilon) = \rho_\sigma(s) \left| \frac{ds}{d\varepsilon} \right| = \varepsilon^{-1} e^{\varepsilon s} \rho_\sigma(s) \quad (34)$$



and becomes for

$$\ln \rho^0(\varepsilon) \approx ts(\varepsilon) - \omega_d \left[ \frac{s(\varepsilon)}{2} \right]^d, \quad s \rightarrow \infty \quad (35)$$

Hence it follows that if  $d > 1$ ,  $\rho^0(\varepsilon)$ , provided that  $|\varepsilon| = \varepsilon_0 = e^{ts_0}$ , where

$$s_0 = \left( \frac{2^d t}{d \omega_d} \right)^{1/(d-1)}$$

has a narrow ( $\sim t^{-(d-2)/2(d-1)}$  wide) maximum

$$\ln \rho^0(\varepsilon) \simeq \frac{d-1}{d} \left( \frac{(2t)^d}{d \omega_d} \right)^{1/(d-1)} \quad (36)$$

and when  $|\varepsilon| \rightarrow 0$  ( $s \rightarrow \infty$ ),  $\rho^0(\varepsilon)$  tends to zero as  $\exp[-\omega_d(s(\varepsilon)/2)^d]$ , that is, there is a gap in the density of states which was predicted by Refs. 1 and 2. Therefore, for large  $s$ , one has to calculate the contribution to the density of states due to the parameter  $t$  being finite, though very large (see Section 8).

In the one-dimensional system ( $d = 1$ ) the density of states at the center of the impurity band has, according to Eqs. (33) and (35), an integrable singularity:

$$\rho^0(\varepsilon) \sim t^{-1} |\varepsilon|^{-1+t^{-1}} \quad (37)$$

and for this reason the above-mentioned contribution is always small. In particular, in the Frish-Lloyd model<sup>(3)</sup> with attraction, in complete agreement with the exact solution,<sup>(4,5)</sup> we obtain from Eq. (37):

$$\rho^0(\varepsilon) \sim c |\varepsilon|^{-1+1/(t|E_0|^{1/2})}, \quad c = (2t)^{-1}$$

It is worth mentioning that a more detailed investigation enables us to detect the asymmetry of the numerical factor predicted by the exact solution.<sup>(4,5)</sup> Indeed, the level  $s \gg 1$ , in the one-dimensional case, can arise from realization of either diagram I3 (Fig. 3) or diagram I4 (Fig. 4). The

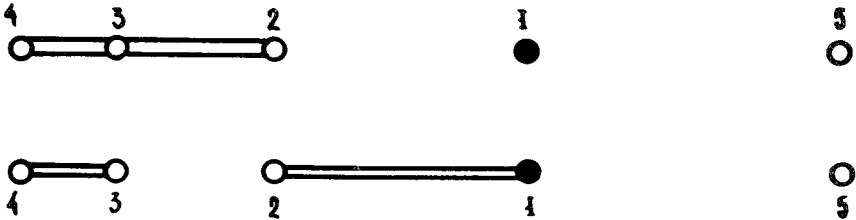


Fig. 3

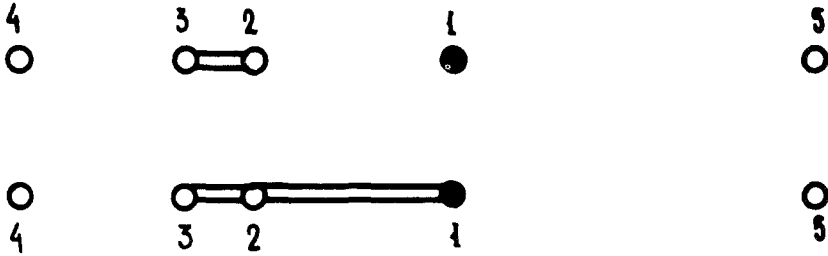


Fig. 4

figures show the rearranging diagram parts and a distant center (5); here  $x_{12} = s/2 \gg 1$ ,  $x_{15} > s/2$ , and  $x_{23} \sim x_{34} \sim 1$ . The diagram in Fig. 3 generates the level  $s$ , the respective  $\varepsilon$  value being  $\varepsilon = 2 |E_0| \exp(-ts)$ , while for the diagram of Fig. 4 the level  $s - 2x_{23} < s$  corresponds to  $\varepsilon = -2 |E_0| \exp(-ts + 2tx_{23})$ . A simple calculation shows that because of such difference, the densities of states  $\rho_+(\varepsilon)$  for  $\varepsilon > 0$  and  $\rho_-(\varepsilon)$  for  $\varepsilon < 0$  are related in the range  $|\varepsilon| \rightarrow 0$  as

$$C\rho_+(|\varepsilon|) = \rho_-(|\varepsilon|)$$

where  $C$  is a certain positive number larger than unity (in the exact solution,  $C = 2$ ).

## 7. DENSITY-DENSITY CORRELATION FUNCTION

Now let us calculate the density-density correlation function, specified by relation

$$p(\mathbf{x}, \mathbf{x}'; \varepsilon, \varepsilon') = \left\langle \sum_{m,p} \psi_p^*(\mathbf{x}) \psi_p(\mathbf{x}') \psi_m^*(\mathbf{x}') \psi_m(\mathbf{x}) \delta(\varepsilon - \varepsilon_p) \delta(\varepsilon' - \varepsilon_m) \right\rangle$$

(in the impurity bands the states are real, and we shall below omit the complex conjugation symbol), and represent it as a sum of the diagonal and nondiagonal terms as follows:

$$p(\mathbf{x}, \mathbf{x}'; \varepsilon, \varepsilon') = \left| \frac{ds}{d\varepsilon} \right|^2 \delta_{\sigma\sigma'} \delta(s - s') p_1(\mathbf{x}, \mathbf{x}'; s, \sigma) + \left| \frac{ds}{d\varepsilon} \frac{ds'}{d\varepsilon'} \right| p_2(\mathbf{x}, \mathbf{x}'; s, \sigma; s', \sigma') \quad (38)$$

Here

$$\begin{aligned}
 p_1(\mathbf{x}, \mathbf{x}'; s, \sigma) &= \left\langle \sum_m \psi_m^2(\mathbf{x}) \psi_m^2(\mathbf{x}') \delta_{\sigma\sigma_m} \delta(s - s_m) \right\rangle \\
 p_2(\mathbf{x}, \mathbf{x}'; s, \sigma; s', \sigma') & \\
 &= \left\langle \sum_{\substack{p,m \\ (p \neq m)}} \psi_p(\mathbf{x}) \psi_p(\mathbf{x}') \psi_m(\mathbf{x}') \psi_m(\mathbf{x}) \delta_{\sigma\sigma_p} \delta_{\sigma'\sigma_m} \delta(s - s_p) \delta(s' - s_m) \right\rangle
 \end{aligned} \tag{39}$$

Consider first  $p_1(\mathbf{x}, \mathbf{x}'; s, \sigma)$  the density–density correlation function for coinciding energies, in the variables  $s, \sigma$ . Passing in Eq. (39) to the limit  $t \rightarrow \infty$  from summation over levels to summation over diagrams, we see that the right-hand side of this equality has the structure of Eq. (12), where

$$F_{\mathfrak{R}} = \begin{cases} \delta_{\sigma\sigma_{\mathfrak{R}}} \delta(s - s_{\mathfrak{R}}) \psi_{\mathfrak{R}}^2(\mathbf{x}) \psi_{\mathfrak{R}}^2(\mathbf{x}') & \text{(I)} \\ \delta(s - s_{\mathfrak{R}}) \psi_{\mathfrak{R}\sigma}^2(\mathbf{x}) \psi_{\mathfrak{R}\sigma}^2(\mathbf{x}') & \text{(II)} \end{cases} \tag{40}$$

The states  $\psi_{\mathfrak{R}}(\mathbf{x})$  (I) and  $\psi_{\mathfrak{R}\sigma}(\mathbf{x})$  (II), in the main approximation, according to Eqs. (8) and (9), have the form (standard denumeration)

$$\psi_{\mathfrak{R}}(\mathbf{x}) = \psi^{(0)}(\mathbf{x} - \mathbf{x}_1) \tag{I}$$

$$\psi_{\mathfrak{R}\sigma}(\mathbf{x}) = 2^{-1/2} [\psi^{(0)}(\mathbf{x} - \mathbf{x}_1) + \sigma \psi^{(0)}(\mathbf{x} - \mathbf{x}_2)] \tag{II}$$

Averaging Eq. (40), taking into account Eqs. (22) and (23), the symmetry of  $\tilde{P}_{\mathfrak{R}}$  for type II diagrams with respect to the first two arguments and the fact that for distances of the order of 1 (the average separation of impurities)  $[\psi^{(0)}(\mathbf{x})]^2 = \delta(\mathbf{x})$ , we have the following for the contributions of I and II diagrams to  $p_1$ :

$$p_1^I = \rho_{\sigma}^I(s) \delta(\mathbf{x} - \mathbf{x}') \tag{41}$$

$$\begin{aligned}
 p_1^{II} &= \frac{1}{2} \rho_{\sigma}^{II}(s) \delta(\mathbf{x} - \mathbf{x}') + \frac{1}{4} \left[ P_{II2}(s) \delta(s - |\mathbf{x} - \mathbf{x}'|) \right. \\
 &\quad \left. + \sum_{\substack{II \\ k > 2 \\ \mathfrak{R}}} \int \{ P_{\mathfrak{R}}(\Gamma_{\mathfrak{R}}) \delta[s - s(\Gamma_{\mathfrak{R}})] \} \Big|_{\mathbf{x}_2 = \mathbf{x}' - \mathbf{x}} d\mathbf{x}_3 \cdots d\mathbf{x}_k \right]
 \end{aligned} \tag{42}$$

$$p_1 = p_1^I + p_1^{II} \tag{43}$$

As regards the nondiagonal part  $p_2$ , it is for  $t \rightarrow \infty$  (i.e., in terms of the geometric systematics of Section 4) contributed to by only the pairs of levels  $n, m$ , referring to the same type II diagram and corresponding to energies of

different signs. The expression for  $p_2$  may also be reduced to the form of Eq. (12); this time,  $F_{\mathfrak{R}}$  is

$$F_{\mathfrak{R}} = \begin{cases} 0 & \text{(I)} \\ \delta_{\sigma, -\sigma'} \delta(s - s') \delta(s - s') \delta(s - s_{\mathfrak{R}}) \psi_{\mathfrak{R}\sigma}(\mathbf{x}) \psi_{\mathfrak{R}\sigma}(\mathbf{x}') \psi_{\mathfrak{R}\sigma'}(\mathbf{x}') \psi_{\mathfrak{R}\sigma'}(\mathbf{x}) & \text{(II)} \end{cases}$$

By averaging these expressions, we obtain for  $p_2$  a result which differs from Eq. (42) by the sign before the square brackets and the presence of a new multiplier of the form  $\delta_{\sigma, -\sigma'} \delta(s - s')$ .

The final result is

$$p(\mathbf{x}, \mathbf{x}'; \varepsilon, \varepsilon') = \left| \frac{ds}{d\varepsilon} \right| \delta(|\varepsilon| - |\varepsilon'|) p(\mathbf{x}, \mathbf{x}'; s; \sigma, \sigma')$$

$$p(\mathbf{x}, \mathbf{x}'; s; \sigma, \sigma') = \delta(\mathbf{x} - \mathbf{x}') [\delta_{\sigma\sigma'} \rho_{\sigma}^I(s) + \frac{1}{2} \rho^{II}(s)]$$

$$+ \frac{(-1)^{(\sigma - \sigma')/2}}{4} \left[ P_{II2}(s) \delta(s - |\mathbf{x} - \mathbf{x}'|) \right.$$

$$\left. + \sum_{\mathfrak{R}}^{II} \int \{ P_{\mathfrak{R}}(\Gamma_{\mathfrak{R}}) \delta[s - s(\Gamma_{\mathfrak{R}})] \} \Big|_{\mathbf{x}_2 = \mathbf{x}' - \mathbf{x}} dx_3 \cdots dx_k \right] \quad (44)$$

Hence we see that the density–density correlation function, in the main approximation ( $t \rightarrow \infty$  after transition to the variables  $s, \sigma$ ) corresponding to the geometric systematics is nonzero only for energies differing by no more than the sign. Being a function of the spatial variables, this correlation function (as  $p_1$  and  $p_2$ ) consists of three terms, two of which are singular and are nonzero only for the points  $\mathbf{x}$  and  $\mathbf{x}'$  which either coincide or are situated at exactly the distance  $s$ . The third summand is a smooth function; however, when  $|\mathbf{x} - \mathbf{x}'| < s$  it is zero. At  $s < |\mathbf{x} - \mathbf{x}'|$  it consists of contributions of peculiar states of type II which collectivize comparatively widely separated centers (see Section 4).

## 8. DENSITY OF STATES AT THE BAND CENTER

Up to now our study has been based on the geometric systematics of levels and states which arises in the limit  $t \rightarrow \infty$ . However, allowance for the finite, though large, value of the  $t$  parameter results in broadening of the boundaries of the  $\Delta\Gamma_i$  regions (see Section 4) and conversion into bridges with a finite thickness  $\sim t^{-1}$  outside which the geometric systematics holds. If the contribution of states it describes becomes small, one has to include that

of the states generated by the small probability configurations belonging to the bridges.

The finiteness of the parameter  $t$  must first of all affect the behavior of the density of states  $\rho(\varepsilon)$  at the band center,  $\varepsilon \rightarrow 0$ , because this quantity calculated in terms of the geometric systematics (34) goes to zero when  $\varepsilon \rightarrow 0$ , according to Eq. (35). We shall consider, as we did in the second half of Section 7, the auxiliary problem with a finite number  $N$  of impurities, assuming that in the system no more than one rarefied fluctuation exists and the largest  $s$  value corresponds to the situation that the largest are the two last terms in Eq. (6) and thus  $s_N$  is given by equation

$$e^{-ts_N} = -\sigma_N \frac{\kappa_N}{\kappa_{N-1}} e^{-t(\bar{L}_N - \bar{L}_{N-1})} \quad (45)$$

In the geometric systematics (i.e., when  $t \rightarrow \infty$ ) the quantities  $\bar{L}_n$  coincide with  $L_n$  perimeters of minimum  $n$ -polygons and therefore large  $s$  arises only on a rarefied fluctuation of a very large radius. However, when  $t$  is finite, another possibility appears, which can be seen, if we write the coefficients  $Q_N$  of Eq. (3) as

$$Q_N = \kappa_N e^{-t\bar{L}_N} = \kappa_N (e^{-t\bar{L}_N} - e^{-t\bar{L}'_N}) \quad (46)$$

Here the first terms arises from a minimum  $N$ -polygon and the other ones whose parity of the number of loops coincides with that of  $\Gamma_N$ , and the second is the contribution of  $N$ -polygons with the number of loops of the opposite parity. Then, Eq. (45) for the maximum root  $s_N$  becomes

$$s_N = (\bar{L}_N - \bar{L}_{N-1}) - t^{-1} \ln\{1 - \exp[-t(\bar{L}'_N - \bar{L}_N)]\} \quad (47)$$

When  $t \rightarrow \infty$ ,  $\bar{L}_N \rightarrow L_N$ , and also  $\bar{L}'_N > \bar{L}_N$ , so that the latter equation reduces to the above equation (7):

$$s_N = L_N - L_{N-1}$$

On the other hand, for finite  $t$ , large  $s$ , as is suggested by Eq. (47), may be provided not only by the first, but also by the second term. This is the case when  $\bar{L}'_N$  and  $\bar{L}_N$  defined by Eq. (46) are anomalously close:  $\bar{L}'_N - \bar{L}_N \sim t^{-1} \exp(-ts_N)$ . The probability of such event is very small, however, for very large  $s$ , it becomes, as we shall see, larger than that of the rarefied fluctuation leading to Eq. (35).

Since, for  $t \rightarrow \infty$ , the  $\bar{L}_N$  and  $\bar{L}'_N$  quantities coincide with the  $L_N$  perimeter of the minimum  $N$ -polygon and the  $L'_N$  perimeter of the minimum  $N$ -polygon with the number of loops of the opposite parity, then resonance coincidence of  $\bar{L}_N$  and  $\bar{L}'_N$  admits of a clear geometric illustration (see Fig. 5

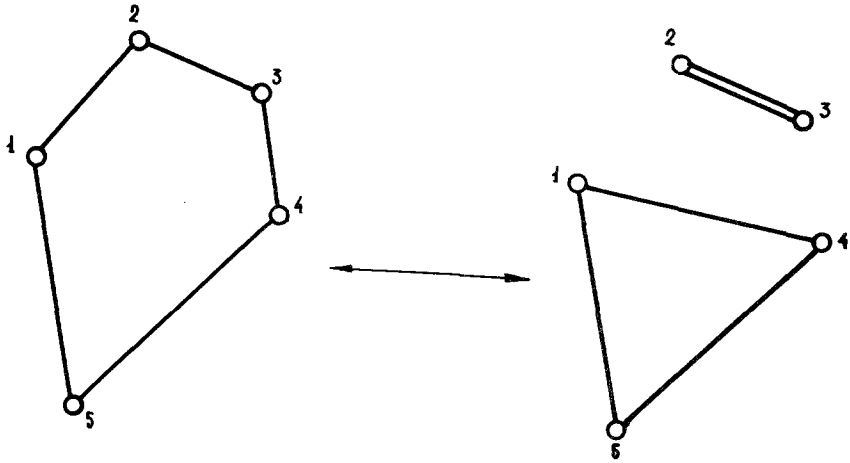


Fig. 5

representing pentagons consisting of one and two loops and having equal perimeters). Actually, however, large  $s$  require coincidence, with exponential accuracy ( $\sim e^{ts - \ln t}$ ) of  $\bar{L}_N$  and  $\bar{L}'_N$  differing from minimum perimeters  $L_N$  and  $L'_N$  by an amount of the order of  $t^{-1}$ . Therefore the configurations under discussion in this section are close to fully degenerated configurations, like that shown in Fig. 5 (though they are not exactly such).

The representation (46) is valid not only for the last, but also for all the preceding coefficients  $Q_n$  with  $n > 4$ , and therefore there may be resonance coincidences of  $\bar{L}_n$  and  $\bar{L}'_n$  ( $n < N$ ), resulting in anomalously small coefficient  $Q_n$  and, on the contrary, anomalously large effective perimeter  $\tilde{L}_n$ . This fact, however, does not affect much the structure of levels and states with  $n < N$  of the auxiliary problem. For one thing, the probability of the resonance coincidence alone is very low. For another, the coincidence, in case of moderately large  $n$ 's, does not, as a rule, lead to appearance of the respective level with  $s \gg 1$ . Indeed, allowance for the finiteness of  $t$  leads first of all to loss of the literal geometric sense of the quantities  $\tilde{L}_n$ , with the whole analysis of Section 3 retained in general outline for large  $t$ . In particular, the process by which the roots of Eq. (6) appear is still described by Fig. 1, the ordinate being, however, the effective perimeter  $\tilde{L}_n$  instead of the true perimeter  $L_n$ . If some effective perimeter  $\tilde{L}_n$  is anomalously large because of  $\bar{L}_n$  and  $\bar{L}'_n$  resonance coincidence, then in the subsequent terms of Eq. (6) with more numbers, the resonance, with overwhelming probability, disappears. This means in Fig. 1 that the point  $(n, \tilde{L}_n)$  does not belong to the convex envelope and does not therefore participate in the spectrum

formation. [Note that the point  $(N, \tilde{L}_N)$  always belongs to the convex envelope.]

When passing from the auxiliary problem to initial (i.e., in the limiting process  $N \rightarrow \infty$ ,  $V \rightarrow \infty$ ,  $V/N \rightarrow l^3$ ), the situation alters. For very large, though still finite,  $t$ , the convex envelope in Fig. 1, in the near- $N$  range of  $n$  corresponding to the last levels with  $s \gg 1$ , is a very rapidly increasing function. The small probability of the level with  $s \gg 1$ , as a result of the resonance coincidence of  $\bar{L}_n \approx \bar{L}'_n$  for  $n \sim N$ , becomes, as we shall see, larger than that of the rarefied fluctuation generating the levels with the same  $s$  value. Therefore, it is the  $\bar{L}_n, \bar{L}'_n$  coincidence for different, though close to  $N$ ,  $n$  values which is responsible for the macroscopic number of levels with  $s \gg 1$  (proportional to  $N$ , for  $N \rightarrow \infty$ ).

The finiteness of  $t$  slightly distorts the quantum states obtained in terms of the main approximation. They continue to be localized mainly at one or two centers, but the coefficients in formulas similar to Eqs. (8) and (9) are somewhat different from 1 and  $2^{1/2}$ , because the right-hand part receives slight admixture of states localized at other centers. Essentially different are the states corresponding to the levels appearing as a result of the  $\bar{L}_n, \bar{L}'_n$  resonance. Here, since the effective perimeter  $\tilde{L}_n$  is formed by all impurity centers, the corresponding state collectivizes a large number of centers.

We have till now discussed the transition  $n - 1 \rightarrow n$ . One would think that a different situation is possible, with the transition  $n - 2 \rightarrow n$  realized. However, as we shall see below, the states forming the density of states at the band center are associated with special configurations, the site of simultaneous realization of the pertinent  $\bar{L}_n, \bar{L}'_n$  resonance and the large radius rarefied fluctuation whose volume at the transition  $n - 2 \rightarrow n$  is essentially larger than that at  $n - 1 \rightarrow n$  and the associated probability essentially smaller.

Now turn to calculation of the density of states  $\rho_\sigma(s, t)$  at the band center ( $s \rightarrow \infty$ ) and introduce the function  $P_\sigma(x, y)$  which is the average of

$$\delta_{\sigma\sigma_N} \delta[x - (\bar{L}_N - \tilde{L}_{N-1})] \delta[y - (\bar{L}'_N - \bar{L}_N)]$$

in the case of  $N - 1 \rightarrow N$  and equals zero in the opposite case. From Eq. (47), we obtain for the density of states that

$$\rho_\sigma(s, t) = \int_0^s dx \int_0^\infty dy \delta[s - x + t^{-1} \ln(1 - e^{-ty})] P_\sigma(x, y)$$

Since  $t \gg 1$ , allowance for the  $t$ -dependent term in the argument of the  $\delta$  function is necessary only for very small values of  $y$ ,  $y \sim t^{-1} e^{-ts}$ . Therefore in the range  $y > y_0$ , where  $y_0$  is of the order of, e.g.,  $t^{-2}$ , this term may be disregarded. By extending then integration to the entire semiaxis  $y$  and iden-

tifying  $\bar{L}_N$  and  $\tilde{L}_{N-1}$  with  $L_N$  and  $L_{N-1}$ , respectively, obtain, to within the magnitudes of the order of  $t^{-1}$ , the contribution to the band center density of states calculated above in Section 6:

$$\rho_\sigma^1(s) = \int_0^\infty P_\sigma(s, y) dy \quad (48)$$

The contribution of resonance configurations with  $\bar{L}'_N \approx \bar{L}_N$  is related to the integral over the small  $y$  range:  $0 < y < y_0$ . By integrating over  $y$ , we have ( $z = s - x$ ):

$$\rho_\sigma^*(s, t) = \rho_\sigma(s, t) - \rho_\sigma^1(s) \approx \int_0^s e^{-tz} P_\sigma(s - z, 0) dz \quad (49)$$

Both the contributions, (48) and (49), are expressed in terms of the same function  $P_\sigma(x, y)$  essentially facilitating the further analysis. Because  $\rho_\sigma^1(s)$  for large  $s$  has the form of Eq. (33)

$$\ln \rho_\sigma^1(s) \approx -2^{-d} \omega_d s^d$$

and the geometric systematics is insensitive to the magnitude of  $y = \bar{L}'_N - \bar{L}_N$  then it is natural to think that  $\ln P_\sigma(x, y)$  has for  $x \rightarrow \infty$  in the main order the same asymptotic value:

$$\ln P_\sigma(x, y) \approx -2^{-d} \omega_d x^d \quad (50)$$

By substituting Eq. (50) into (49) and allowing for the relation [see Eq. (34)]

$$\rho(\varepsilon) = t^{-1} e^{t\varepsilon} \rho_\sigma(s, t)$$

obtain

$$\ln \rho(\varepsilon) = t\varepsilon + \ln \rho_\sigma(s, t) = \begin{cases} t\varepsilon - 2^{-d} \omega_d s^d, & 1 \ll s \leq s_0 \\ \frac{d-1}{d} \left( \frac{(2t)^d}{d\omega_d} \right)^{1/(d-1)}, & s_0 \leq s \end{cases} \quad (51)$$

Thus, the density of states  $\rho(\varepsilon)$  for  $s \gg 1$  up to  $s = s_0$  is governed by states given by the geometric systematics, realized at rarefied fluctuations of an ever increasing (with  $s$ ) volume and localized at the impurity situated at the center of the volume. For  $s > s_0$  (in the vicinity of the gap predicted by the geometric systematics) the main energy-independent (with logarithmic accuracy) contribution to the density of states  $\rho_\sigma(s, t)$  is due to the term  $\rho_\sigma^*(s, t)$ . The corresponding configurations are also associated with rarefied fluctuations; however, now the fluctuation radius is fixed,  $\bar{L}_N - \tilde{L}_{N-1} = s_0$



and the  $s$  increase is only due to increasingly close coincidence of  $\bar{L}'_N$  and  $\bar{L}_N$ . The gap in the density of states  $\rho^0(\varepsilon)$  is partially filled; still  $\rho(\varepsilon)$  has a minimum at  $\varepsilon \rightarrow 0$ , though [see Eq. (36)]

$$\ln \rho(0) \approx \ln \rho_\sigma^*(\infty, t) \approx \ln \rho^0(\varepsilon_0)$$

The states filling up the gap, as has been said, collectivize a large number of centers.

## 9. GENERAL SPECTRUM STRUCTURE

With the results obtained above, we can describe the impurity band spectrum structure (see Fig. 6). To begin with, let us discuss the case of low concentration,  $c \ll c_{cr}$  ( $t \gg 1$ ), where all states are localized (such states are shown as the shaded area in Fig. 6). Near the boundaries  $\varepsilon_g$  and  $\bar{\varepsilon}_g$  the spectrum is produced by macroscopic fluctuations (see, e.g., Ref. 6). As  $|\varepsilon|$  decreases, we gradually go into the cluster region associated with dense fluctuations, where a small number (2, 3) of centers are spaced by distances much smaller than the average,  $l$ . This area may be investigated by expansion in the concentration  $c \sim t^{-d}$ .<sup>(1,2)</sup> Still smaller values,  $|\varepsilon| \sim |\varepsilon(l)|$  correspond to states described by the geometric systematics. Their density

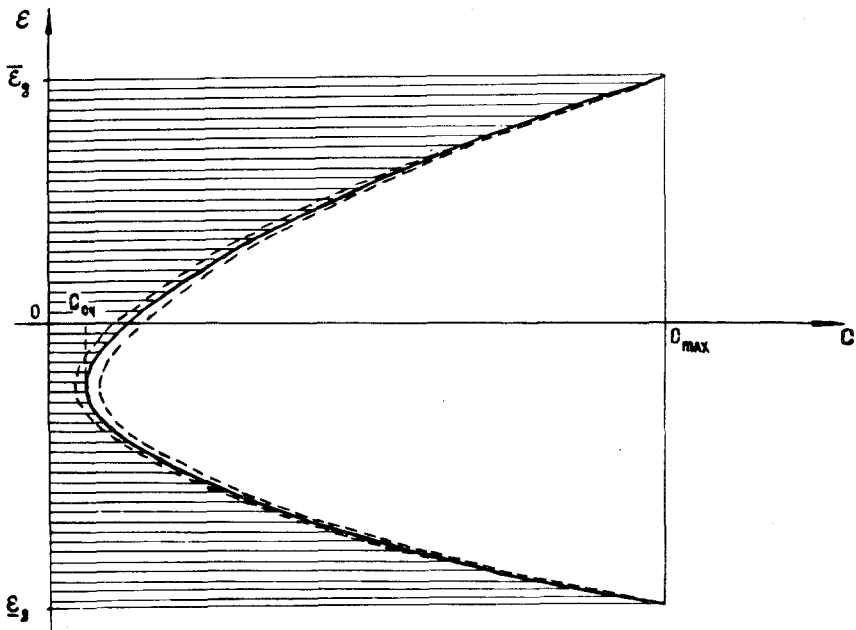


Fig. 6

for  $s \gg 1$  is given by Eq. (33). Finally, in the closest vicinity of the point  $\varepsilon = 0$  the main role belongs to collectivized states which are realized on resonance configurations considered above in Section 8. The width of this region is in the logarithmic scale of the order of  $t^{-d/(d-1)}$  and, as dimension  $d$  increases, tends to the whole spectrum width which in the same scale is  $t^{-1}$ . This is quite natural since with increasing dimension of the space, delocalization becomes easier. In the vicinity of the curve  $c = c_{cr}(\varepsilon)$  separating localized and delocalized states (area bounded by two broken lines in Fig. 6), where fluctuational effects must dominate, one can hardly indicate any method characterized by a finite number of parameters to describe the state. The situation there seems to be much the same as in the vicinity of the II order phase transition point (scaling region) or in a turbulent liquid, where fluctuations are developed so highly that in all scales of an infinite hierarchy the picture of the phenomenon is practically the same.

The initial stage of development of delocalized (extended) states outside the immediate neighborhood of the band center may be analyzed by Eq. (6) describing the level distribution in the auxiliary  $N$ -center problem. The case is possible of coincidence, to within  $t^{-1}$ , of successive differences of minimum perimeters

$$L_{n+1} - L_n \approx L_n - L_{n-1} \approx (\dots)$$

or

$$L_{n+2} - L_n \approx L_n - L_{n-2} \approx (\dots)$$

Then, with certain  $s$  value, several terms of expansion of determinant (2) are of the same order simultaneously, suggesting appearance of multiple roots (with logarithmic accuracy) of Eq. (6). If, in addition, the rearranging parts of contours intersect, then the states involved, unlike in the situation considered in the end of Section 5, collectivize all the rearranging centers.

We deal here in fact with origination of periodical center arrangement. Indeed, it is in the periodical case that special-type resonance situations arise, associated with coincidence of distances  $x_{ik}, x_{kl}, \dots$  between successive pairs of centers, which then leads to smooth level distribution in the band and complete collectivization of states.

Such states have low density, because the portion of the "degenerate" configurations is of the order of  $t^{-k}$ , as defined by the width of the bridges discussed in the beginning of Section 8 (the exponent  $k$  is due to multiplicity of degeneracy of the respective  $s$  root). Their contribution to many-point correlation functions, however, can be essential. In particular, the  $n$ -point correlation function ( $n > 2$ ) is a sum of singular terms containing from one to  $(n - 1)$   $\delta$  functions [cf. Eq. (44)] and a slowly varying term. The terms

with the  $(n-1)$  and  $(n-2)$   $\delta$  functions are generated by the geometric systematics and do not depend on the concentration, while the rest of them are associated with degenerate states and are proportional to  $t^{-k}$ , where  $(n-2-k)$  is the number of  $\delta$  functions. In particular, the slowly varying terms is proportional to  $t^{-(n-2)}$ .

In case of low concentration ( $t \gg 1$ ) the slow terms in the many-point correlation functions are also small, because they consist of contributions of small probability chains of resonance-percolation paths having all the links, to within  $t^{-1}$ , equal. Such a chain is only realized with finite probability, when  $t < t_{cr}$ , where  $t_{cr}$  is the concentration boundary of mobility (state delocalization).

The parameter  $t$  above defines simultaneously all the significant characteristics. On one hand, the overlapping integral for medium distances  $J \sim e^{-t}$  responsible for tunneling between centers estimates the energy region where state delocalization is in principle possible (through development of an infinite cobweblike resonance-percolation net, built up on impurity atoms). On the other hand,  $t^{-1}$ , when  $t \gg 1$ , defines the order of magnitude of possible fluctuations of the net mesh sizes and, consequently, the net relative phase volume tends to zero in the limit  $V \rightarrow \infty$ . As  $t$  decrease (i.e., concentration  $c \sim t^{-d}$  increases), the number of centers in the volume  $k_0^{-d}$  equal to  $c\omega_d$  grows and, when  $\omega_d t^{-d} \gg 1$  ( $d \geq 3$ ), there appears a band of delocalized states, which is why the mobility boundary estimate in this model is  $t_{cr} \sim 1$ .

Thus, for  $c > c_{cr}$  ( $t < t_{cr}$ ), in a certain vicinity of the local level the states are delocalized. However, the spectrum near the boundaries has a fluctuational nature. As the concentration increases, the delocalized state region becomes broader and when  $c_{max} - c \ll c_{max}$  (here  $c_{max}$  is the maximum impurity center concentration corresponding to a completely ordered system) the fluctuation levels fill up only minor vicinities of both the boundaries. Finally, for  $c = c_{max}$  all states are evidently delocalized.

## REFERENCES

1. I. M. Lifschitz, *Zh. Eksp. Teor. Fiz.* **44**:1723 (1963).
2. I. M. Lifschitz, *Usp. Fiz. Nauk* **83**:617 (1964) [*Adv. Phys.* **13**:483 (1964)].
3. H. L. Frish and S. R. Lloyd, *Phys. Rev.* **120**:1179 (1960).
4. J. Morrison, *J. Math. Phys.* **3**:1023 (1962).
5. Yu. A. Bychkov and A. M. Dykhne, *Zh. Eksp. Teor. Fiz.* **51**:1923 (1966).
6. I. M. Lifschitz, S. A. Gredeskul, and L. A. Pastur, *Fiz. Nizk. Temp.* **2**:1093 (1976) [*Sov. J. Low Temp. Phys.* **2**:533 (1976)].